Describing first-order spatio-temporal distortions in ultrashort pulses using normalized parameters

Pablo Gabolde, Dongjoo Lee, Selcuk Akturk and Rick Trebino

Georgia Institute of Technology, 837 State St NW, Atlanta GA 30332 USA
Pablo.Gabolde@physics.gatech.edu

http://www.physics.gatech.edu/frog

Abstract: We develop a first-order description of spatio-temporal distortions in ultrashort pulses using normalized parameters that allow for a direct assessment of their severity, and we give intuitive pictures of pulses with different amounts of the various distortions. Also, we provide an experimental example of the use of these parameters in the case of spatial chirp monitored in real-time during the alignment of an amplified laser system.

OCIS codes: (320.5550) Pulses; (320.7100) Ultrafast measurements.

References and links

1. C. B. Schaffer, A. Brodeur, J. F. García, and E. Mazur, "Micromachining bulk glass by use of femtosecond laser pulses with nanojoule energy," Opt. Lett. **26**, 93-95 (2001).
2. W. Denk, J. H. Strickler, and W. W. Webb, "Two-Photon Laser Scanning Fluorescence Microscopy," Science **248**, 73-76 (1990).
3. R. L. Fork, O. E. Martinez, and J. P. Gordon, "Negative dispersion using pairs of prisms," Opt. Lett. **9**, 150-152 (1984).
4. J.-C. M. Diels, J. J. Fontaine, I. C. McMichael, and F. Simoni, "Control and measurement of ultrashort pulse shapes (in amplitude and phase) with femtosecond accuracy," Appl. Opt. **24**, 1270-1282 (1985).
5. R. Trebino, K. W. DeLong, D. N. Fittinghoff, J. N. Sweetser, M. A. Krumbuegel, and D. J. Kane, "Measuring Ultrashort Laser Pulses in the Time-Frequency Domain Using Frequency-Resolved Optical Gating," Rev. Sci. Instrum. **38**, 3277-3295 (1997).
6. P. O'Shea, M. Kimmel, X. Gu, and R. Trebino, "Highly simplified device for ultra-short measurement," Opt. Lett. **26**, 932-934 (2001).
7. S. Akturk, M. Kimmel, P. O'Shea, and R. Trebino, "Measuring spatial chirp in ultrashort pulses using single-shot Frequency-Resolved Optical Gating," Opt. Express **11**, 68-78 (2003).
8. S. Akturk, M. Kimmel, P. O'Shea, and R. Trebino, "Measuring pulse-front tilt in ultrashort pulses using GRENOUILLE," Opt. Express **11**, 491-501 (2003).
9. C. Dorrer, E. M. Kosik, and I. A. Walmsley, "Spatio-temporal characterization of the electric field of ultrashort pulses using two-dimensional shearing interferometry," Applied Physics B (Lasers and Optics) **74 [Suppl.]**, S209-S217 (2002).
10. C. Dorrer, and I. A. Walmsley, "Simple linear technique for the measurement of space-time coupling in ultrashort optical pulses," Opt. Lett. **27**, (2002).
11. K. Varju, A. P. Kovacs, G. Kurdi, and K. Osvay, "High-precision measurement of angular dispersion in a CPA laser," Appl. Phys. B **Suppl.**, 259-263 (2002).
12. M. Kempe, U. Stamm, B. Wilhelmi, and W. Rudolph, "Spatial and temporal transformation of femtosecond laser pulses by lenses and lens systems," J. Opt. Soc. Am. B **9**, 1158-1165 (1992).
13. X. Gu, S. Akturk, and R. Trebino, "Spatial chirp in ultrafast optics," Opt. Commun. **242**, 599-604 (2004).
14. A. G. Kostenbauder, "Ray-Pulse Matrices: A Rational Treatment for Dispersive Optical Systems," IEEE J. Quantum Electron. **26**, 1148-1157 (1990).
15. S. Akturk, X. Gu, P. Gabolde, and R. Trebino, "The general theory of first-order spatio-temporal distortions of Gaussian pulses and beams," Opt. Express **13**, 8642-8661 (2005).
16. R. V. Hogg, and A. Craig, *Introduction to Mathematical Statistics* (Prentice Hall, 1994).

#77118 - $15.00 USD Received 15 November 2006; revised 15 December 2006; accepted 18 December 2006

17. K. Osvay, A. P. Kovács, Z. Heiner, G. Kurdi, J. Klebniczki, and M. Csatári, "Angular Dispersion and Temporal Change of Femtosecond Pulses From Misaligned Pulse Compressors," IEEE J. Sel. Top. Quant. Electron. **10**, 213-220 (2004).
18. L. Cohen, *Time-frequency analysis* (Prentice Hall, 1995).
19. Z. Bor, and B. Racz, "Group velocity dispersion in prisms and its application to pulse compression and travelling-wave excitation," Opt. Commun. **54**, 165-170 (1985).
20. S. Akturk, X. Gu, E. Zeek, and R. Trebino, "Pulse-front tilt caused by spatial and temporal chirp," Opt. Express **12**, 4399-4410 (2004).

1. Introduction

Ultrashort-pulse lasers are carefully designed to generate the shortest possible pulses, as this is highly desirable in most experimental situations, from micro-machining to multi-photon microscopy [1, 2]. Unfortunately, in propagating through materials, different frequencies ω experience different group delays $\tau(\omega)$, so all transmissive optical components broaden and chirp pulses. Fortunately, pulse compressors can compensate for this group-delay dispersion (GDD) [3]. But, in order to operate, pulse compressors (as well as shapers and stretchers) deliberately rely on an array of *spatio-temporal distortions*, which include angular dispersion, spatial chirp, pulse-front tilt, and angular delay, to name a few. While in theory perfect alignment of a compressor guarantees that the output pulse is free of any of these distortions, in practice residual distortions are often present.

Fortunately, measurement techniques for temporal chirp have been available for decades [4-6], but convenient diagnostics for most spatio-temporal distortions are just now becoming available [7-11]. As a result, while pulse chirp is well understood, the various spatio-temporal distortions that can occur in ultrashort pulses are not so well understood. Such distortions are as detrimental to experiments as chirp, especially when the pulse is focused onto a sample [12]. So an understanding of them is critical. And such an understanding must begin with a common language with which to discuss them.

Unfortunately, such a language does not currently exist. Consider, for example, the case of spatial chirp. Spatial chirp is a coupling between x and ω and corresponds to a variation of the beam center vs. frequency that can be characterized by the derivative $\mathrm{d}x/\mathrm{d}\omega$ (called spatial dispersion) to first order. But spatial chirp may equally well be described by a variation in the center frequency vs. position, and hence the derivative $\mathrm{d}\omega/\mathrm{d}x$ (called frequency gradient), and these two derivatives are not reciprocal [13]. To further complicate matters, some authors use the frequency υ rather than the angular frequency ω [14], and others prefer the wavelength λ. As a result, spatial chirp measurements alone can be reported using *six different derivatives*, all with different units. Worse, it is difficult to estimate the *severity* of spatial chirp from any of these quantities, and how much – or how little – it may eventually affect the performance of an ultrafast system. The cases of pulse-front tilt, angular dispersion, and angular delay are similar. To first order they can be described, respectively, by the derivatives $\mathrm{d}t/\mathrm{d}x$, $\mathrm{d}k_x/\mathrm{d}\omega$, and $\mathrm{d}k_x/\mathrm{d}t$. Or they can be described by the several additional analogous definitions. Thus studies of other spatio-temporal distortions suffer from the same problems.

In this paper we propose an intuitive formalism to describe spatio-temporal distortions. Rather than using first-order derivatives, we rely on normalized correlation parameters that we recently introduced in the context of perfect Gaussian pulses and beams [15]. We also show that such normalized parameters are well adapted to experimental situations where the spatio-temporal distortions of pulses and beams of arbitrary profiles must be minimized in real time.

2. Formal definitions of spatial chirp and other spatio-temporal couplings

We begin by recalling the formal definitions of the above-mentioned normalized spatio-temporal couplings that we briefly introduced recently [15] and that are the subject of this

#77118 - $15.00 USD Received 15 November 2006; revised 15 December 2006; accepted 18 December 2006

paper. We consider first (horizontal) spatial chirp, a coupling in the x–ω domain. Generalization to the other spatio-temporal couplings, namely pulse-front tilt, angular dispersion, and angular delay, is immediate by considering the x–t, k_x–ω and k_x–t domains. Extension to the y coordinate is also immediate.

We call $I(x,\omega) \equiv |E(x,\omega)|^2$ the (spatio-spectral) intensity distribution of the pulse, where x and ω are measured with respect to the beam center and the carrier frequency (that is, have the mean position and mean frequency subtracted off). The intensity $I(x,\omega)$ is normalized such that its integral over space and frequency is 1. We now define the normalized spatial chirp parameter $\rho_{x\omega}$ as the first mixed moment of $I(x,\omega)$, divided by the global beam size Δx and the global bandwidth $\Delta\omega$:

$$\rho_{x\omega} \equiv \frac{\iint dx\, d\omega\, I(x,\omega)\; x\omega}{\Delta x \Delta\omega}$$
$$\text{where } \Delta x \equiv \left[\iint dx d\omega I(x,\omega) x^2\right]^{1/2} \tag{1}$$
$$\text{and } \Delta\omega \equiv \left[\iint dx d\omega I(x,\omega) \omega^2\right]^{1/2}$$

Analogous quantities can be defined for the other first-order spatio-temporal distortions (see section 5).

This definition of spatial chirp as a linear correlation coefficient is applicable to pulses of arbitrary profiles [16], and is consistent with the frequency gradient $d\omega/dx$ and spatial dispersion $dx/d\omega$ parameters introduced in Ref. 15 for Gaussian pulses, in the sense that:

$$\rho_{x\omega} = \frac{\Delta x}{\Delta\omega}\frac{d\omega}{dx} = \frac{\Delta\omega}{\Delta x}\frac{dx}{d\omega} \tag{2}$$

Note that since $\rho_{x\omega}$ is calculated from $|E(x,\omega)|^2$, it does not include a coupling between x and ω that may appear in the *phase* of $E(x,\omega)$. This coupling essentially amounts to angular dispersion [15], and is treated in section 5.

There are numerous properties of this correlation coefficient that make it an attractive choice from a practical point of view:

(1) It is an extension to arbitrary pulses and beams that is consistent with previous definitions of frequency gradient and spatial dispersion.
(2) It is symmetric: when $I(x,\omega)$ is recorded using a camera, it does not matter whether the position axis is vertical and the frequency axis horizontal, or vice-versa.
(3) It is scale-invariant: except for a possible change of sign, it is unaffected by the transformations $x \rightarrow \alpha x$ or $\omega \rightarrow \beta\omega$. Thus, beam magnification does not affect the result. An important practical implication is that experimental trace need not be calibrated: the variables x and ω can represent pixel numbers on a camera, and not necessarily physical quantities with proper units.
(4) It is a dimensionless number.
(5) Because $\rho_{x\omega}$ can be identified with the linear correlation of the joint distribution $I(x,\omega)$ [16], it is even possible to show that:

$$-1 < \rho_{x\omega} < 1. \tag{3}$$

#77118 - $15.00 USD Received 15 November 2006; revised 15 December 2006; accepted 18 December 2006

(6) Conveniently, $\rho_{x\omega} = 0$ corresponds to the absence of the distortion to first order, while an increased value of $|\rho_{x\omega}|$ indicates an increase in the magnitude of spatial chirp (see Fig. 1).

(7) The sign of $\rho_{x\omega}$ simply reveals whether the beam center position increases or decreases with ω.

(8) Also, for all but near-single-cycle pulses, the change from frequency ω to wavelength λ is a linear transformation: $\lambda = -\lambda_0^2\omega/(2\pi c)$; again, λ is measured with respect to the central wavelength λ_0. Written in this form, the change from ω (or υ) to λ is just a change of scale and sign, and therefore:

$$\rho_{x\lambda} = -\rho_{x\nu} = -\rho_{x\omega} \tag{4}$$

(9) Finally, $\rho_{x\omega}$ is equal to the *eccentricity* of an elliptical beam caused by spatial chirp.

To see that the last statement is true, consider a collimated beam with an initial circular beam profile going through an optical device that introduces spatial chirp in the x direction (for example, a misaligned stretcher). We take the input beam to have the same size in the x and y directions: $\Delta x = \Delta y$. Because of spatial chirp, the size of the output beam in the x direction increases to $\Delta x'$. The output beam is therefore elliptical, and can be characterized by its eccentricity e_{xy}:

$$e_{xy} = \sqrt{1 - \frac{\Delta y^2}{\Delta x'^2}} = \sqrt{1 - \frac{\Delta x^2}{\Delta x'^2}}, \quad 0 \le e_{xy} < 1 \tag{5}$$

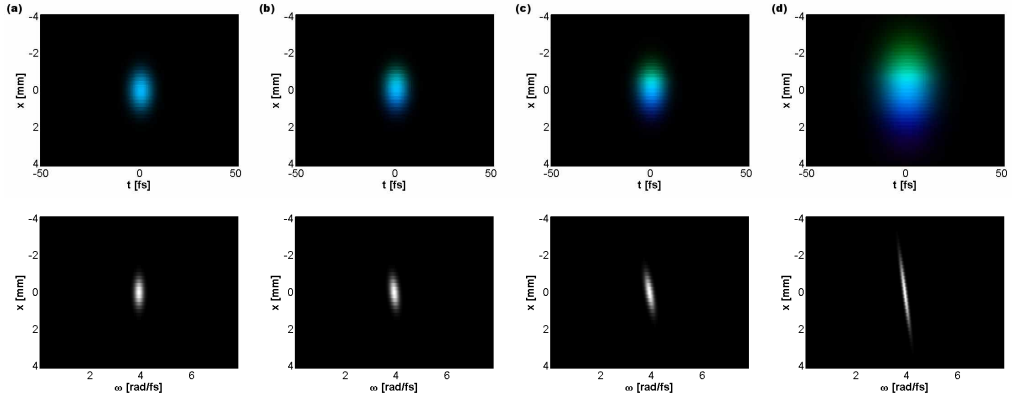

Fig. 1. Profiles of an ultrashort pulse with increasing amounts of spatial chirp, and hence with increasing values of $\rho_{x\omega}$. Upper row: spatio-temporal profiles. The pulses have a central wavelength of 480 nm, and 35 nm of bandwidth. Lower row: corresponding profiles of $I(x,\omega)$, from which $\rho_{x\omega}$ is calculated. (a) $\rho_{x\omega} = 0.00$. (b) $\rho_{x\omega} = 0.30$. (c) $\rho_{x\omega} = 0.60$. (d) $\rho_{x\omega} = 0.90$.

Comparing Eq. (5) with Eq. (45) in Ref. 15, we see that $|\rho_{x\omega}| = e_{xy}$. Although it is easy and intuitive to *think* of $\rho_{x\omega}$ in terms of the eccentricity of the spatial profile, for precise measurements it is preferable to rely on $\rho_{x\omega}$ obtained from the intensity distribution $I(x,\omega)$. In addition, note that if spatial chirp results in a spatial broadening of the beam, and therefore in an elliptical beam, it also results in a *temporal* broadening of the pulse, because of the decrease of available bandwidth at each point x in the beam. Thus, in the presence of spatial chirp, the duration of a pulse with a flat spectral phase does *not* reach its Fourier limit, as can be clearly seen on Fig. 1(d).

#77118 - $15.00 USD Received 15 November 2006; revised 15 December 2006; accepted 18 December 2006

As a side note we would like to point out that the correlation parameter $\rho_{x\omega}$ – and more generally any correlation coefficient ρ that appears in this paper – is very sensitive to small amounts of spatio-temporal coupling, but saturates to a near-unity value for extremely large amounts of coupling (this situation is explored in more details in section 5).

3. Experimental determination of $\rho_{x\lambda}$ and $\rho_{y\lambda}$

We now present a simple arrangement (Fig. 2) that we used to measure the intensity distributions $I(x,\lambda)$ and $I(y,\lambda)$, and we show how to calculate $\rho_{x\lambda}$ and $\rho_{y\lambda}$ from experimental data.

The beam under test is first dispersed in the horizontal plane by a diffraction grating G_1, and the diffracted order $m_1 = 1$, focused by a cylindrical lens, illuminates a digital camera. Simultaneously, the specular reflection ($m_1 = 0$) from G_1 is sent onto a second grating G_2 that disperses the beam *vertically* in a Littrow configuration so that all the beams of interest are contained in the same horizontal plane; the first order ($m_2 = -1$) of G_2 is focused by a second cylindrical lens and illuminates the same digital camera. By blocking the order $m_1 = 1$ from G_1, the camera records $I(x,\lambda)$, while by blocking the order $m_1 = 0$, the camera records $I(y,\lambda)$.

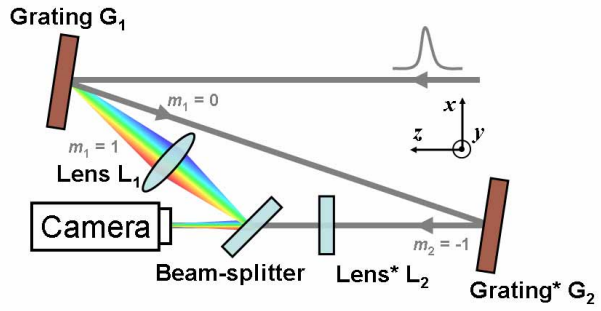

Fig. 2. Apparatus used to record $I(x,\lambda)$ and I(y,λ). **G_1** diffraction grating (dispersing in plane); **L_1** cylindrical lens (collimating in plane); **G_2** diffraction grating (in Littrow, dispersing out of plane); **L_2** cylindrical lens (collimating out of plane).

Once the two images have been recorded, extracting the parameter $\rho_{x\lambda}$ and $\rho_{y\lambda}$ from $I(x,\lambda)$ and $I(y,\lambda)$ is a direct application of Eq. (1), as long as the integrals are replaced by discrete sums. As stated in section 2, it is not necessary to calibrate the axes of the digital camera: x, y and λ can simply refer to pixel numbers. Additionally, we use the fact that the wavelength axis can be either horizontal or vertical. However, Eq. (1) does require that the function $I(x,\lambda)$ be centered with respect to its axes. When pixel numbers are used, this is never the case, and therefore it is easier to rewrite Eq. (1) in the case of un-centered, discrete distributions. To do so, we first introduce the moments μ_{pq} of the intensity distribution $I(x,\lambda)$:

$$\mu_{pq} \equiv \sum_{x,\lambda} I(x,\lambda) x^p \lambda^q \tag{6}$$

The spatial chirp parameter $\rho_{x\lambda}$ is then computed using the following equation, which is a convenient form of Eq. (1) that does not require the data $I(x,\lambda)$ to be centered:

$$\rho_{x\lambda} = \frac{\mu_{11} - \mu_{01}\mu_{10}}{\left[\mu_{20} - \mu_{10}^{\,2}\right]^{1/2}\left[\mu_{02} - \mu_{01}^{\,2}\right]^{1/2}} \tag{7}$$

#77118 - $15.00 USD Received 15 November 2006; revised 15 December 2006; accepted 18 December 2006

Note that some devices are able to detect spatial chirp without the complete measurement of $I(x,\lambda)$ [7]. In that case the spatial chirp parameter $\rho_{x\lambda}$ may be calculated using Eq. (2) instead.

Because Eq. (7) involves sums on the entire image, it is likely to include various background effects, such as scattered light or thermal noise, that might affect the recorded image, in particular in regions where the intensity $I(x,\lambda)$ is low. To mitigate these effects, it is desirable to apply a threshold to $I(x,\lambda)$ before calculating $\rho_{x\lambda}$, by setting to 1 any values of the intensity that are above a pre-defined threshold, and setting the others to 0 (see Fig. 3 for an example). As a simple alternative, it is possible to let the camera saturate a large portion of the trace, and only retain the saturated values (i.e., setting non-saturated values to zero) before applying Eq. (7). We found both methods to be consistent and equivalently robust to noise, and numerical simulations show that they yield the same result as a direct application of Eq. (7).

In summary, Eq. (6) and (7) are a simple, efficient and robust method to calculate $\rho_{x\lambda}$. This procedure is extremely well adapted to data-processing computer programs like MATLAB, and allows easy monitoring of the spatial chirp in real time during the alignment of complex ultrafast laser systems.

4. Experimental results

We applied this method to monitor spatial chirp as we aligned a mode-locked Ti:Sapphire laser with an external pulse compressor seeding a chirped-pulse amplifier (CPA). The apparatus was set up as described above, and images were captured by a 1024×728 Firewire digital camera (Sony XCD-710) directly in MATLAB where the parameters $\rho_{x\lambda}$ and $\rho_{y\lambda}$ were calculated and displayed in real time.

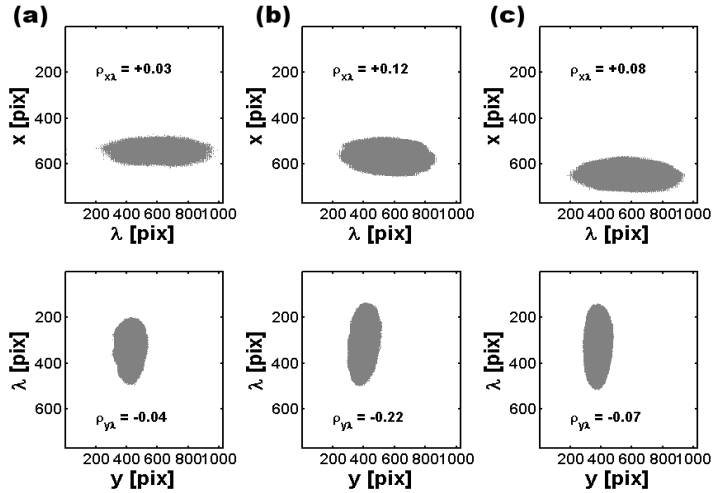

Fig. 3. Typical raw experimental data obtained during real-time monitoring of a Ti:Sapphire oscillator and its external prism pulse compressor, showing the parameters $\rho_{x\lambda}$ (top row) and $\rho_{y\lambda}$ (bottom row) obtained after applying a threshold on the measured images. (a) Oscillator output before the external pulse compressor. (b) External pulse compressor output, misaligned in the vertical plane. (c) External pulse compressor output, adjusted in the vertical plane.

We should point out that, in this work, we chose to monitor spatial chirp as an example; of course, it is well known that spatio-temporal distortions from a stretcher or a compressor arise from residual angular dispersion [17]. However, as the pulse emerging from these devices propagates in free space, angular dispersion results in spatial chirp, and minimizing spatial chirp in the far field amounts to minimizing residual angular dispersion.

#77118 - $15.00 USD Received 15 November 2006; revised 15 December 2006; accepted 18 December 2006

To ensure a proper alignment of the gratings and cylindrical lenses in the setup, we used a reference pulse that was spatially filtered using a single-mode fiber. We then monitored the values of spatial chirp along x and y as we aligned the system (Fig. 3). Table 1 shows typical values of spatial chirp that we found during this procedure. A misaligned stretcher exhibits typical values of ρ = 0.50–0.60, and occasionally values as high as 0.80 or 0.90. Realignment of a retro-reflector inside the unit brought ρ to values typically below 0.20. Even smaller values are obtained after amplification and re-compression, which we attribute to the spectral clipping that happens in our compressor unit. During these alignment procedures, beam pointing changes resulted in deviations of $\rho_{x\lambda}$ on the order of 0.01, which can be roughly considered as the experimental detection limit of our setup.

Table 1. Typical values of spatial chirp measured in different ultrafast optical systems.

Laser system	$\lvert\rho_{x\lambda}\rvert$	$\lvert\rho_{y\lambda}\rvert$
Ti:Sapphire oscillator (spatially filtered)	<0.01	<0.01
Ti:Sapphire oscillator	<0.05	<0.05
Ti:Sapphire oscillator (with an external pulse compressor)	0.05–0.10	0.05–0.10
Misaligned pulse stretcher in a CPA	0.20–0.50	~0.60
Realigned pulse stretcher in a CPA	0.20	<0.01
CPA output pulse (stretched, amplified, recompressed)	0.05–0.20	0.05–0.20

5. Analogy with pulse broadening in dispersive media and extension to other spatio-temporal distortions

There is a perfect analogy between the effects due to dispersion, and those due to spatio-temporal distortions. The first-order cause of pulse broadening due to dispersion is often characterized by the group-delay dispersion, $d\tau/d\omega$, although this can also be considered as a temporal variation of the instantaneous frequency ω_{inst} at a constant rate $d\omega_{inst}/dt$. In analogy with Eq. (2), it is possible to define a temporal chirp parameter $\rho_{\omega t}$, normalized by the pulse duration Δt and the bandwidth $\Delta\omega$, and that satisfies:

$$\rho_{\omega t} = \frac{\Delta t}{\Delta \omega}\frac{d\omega_{inst}}{dt} = \frac{\Delta \omega}{\Delta t}\frac{d\tau}{d\omega} \tag{8}$$

The temporal chirp parameter $\rho_{\omega t}$ can also be defined in a form similar to Eq. (1) by considering the Wigner distribution of the pulse $I_W(\omega,t)$. As an example, consider a chirped Gaussian pulse with a bandwidth $\Delta\omega$ and a group-delay dispersion $d\tau/d\omega$:

$$E(\omega) = E_0 \exp\left[-\frac{\omega^2}{4\Delta\omega^2} + \frac{i}{2}\frac{d\tau}{d\omega}\omega^2\right] \tag{9}$$

The Wigner distribution of this pulse is given by [18]:

$$I_W(\omega,t) \propto \left|E_0\right|^2 \exp\left[-\frac{\omega^2}{2\Delta\omega^2} - \frac{\left(t-\left(d\tau/d\omega\right)\omega\right)^2}{1/\left(2\Delta\omega^2\right)}\right] \tag{10}$$

Note the presence of the coupling term $t - (d\tau/d\omega)\omega$, whose ω-dependent term becomes important when $d\tau/d\omega \neq 0$ (i.e., $\rho_{\omega t} \neq 0$), and which is similar to the coupling term, $x - (dx/d\omega)\omega$, that arises in the case of spatial chirp ($\rho_{x\omega} \neq 0$).

#77118 - $15.00 USD Received 15 November 2006; revised 15 December 2006; accepted 18 December 2006

It is very instructive to consider the relation between $\rho_{\omega t}$ and the pulse duration Δt because dispersion effects are easily and intuitively interpreted in the time domain. Figure 4(a) shows the dependence of the pulse duration (normalized to its Fourier limit) with $\rho_{\omega t}$. It is obvious that the parameter $\rho_{\omega t}$ is very sensitive to *small amounts of dispersion*: a value of $\rho_{\omega t}$ = 0.30 corresponds to a pulse stretched by only 5%, which is acceptable in many situations. On the other hand, very large stretching ratios, such as those obtained by pulse stretchers in CPA systems, correspond to values of $\rho_{\omega t}$ very close to 1, and rapidly become indistinguishable. Thus, these correlation coefficients are ideal for monitoring ultrafast systems that must approach the Fourier limit, but less than ideal for cases in which one is deliberately attempting to introduce massive amounts of these distortions.

In this respect, it is also interesting to compare the normalized parameters that we introduce here with another normalized parameter that was proposed for the study of spatio-temporal distortions in general: the *degree of spatio-temporal uniformity* μ [10]. This parameter is calculated from the spatially and spectrally resolved electric field *amplitude*:

$$\mu \equiv \frac{\iint d\omega_1 d\omega_2 \left| \int dx\, E(x,\omega_1) E^*(x,\omega_2) \right|^2}{\left[\iint dx\, d\omega \left| E(x,\omega) \right|^2 \right]^2} \tag{11}$$

The degree of spatio-temporal uniformity μ may be measured experimentally using linear techniques, and it describes *all* possible spatio-temporal couplings, which can be convenient in some cases: μ = 1 corresponds to a pulse free of spatio-temporal distortions, while $0 < \mu < 1$ indicates that some distortions are present. However, the parameter μ is not very sensitive to small amounts of spatio-temporal distortions. As shown in Fig. 4(b) in the case of spatial chirp, there is little change in μ in the region of small distortions ($\rho_{x\omega} \approx 0$).

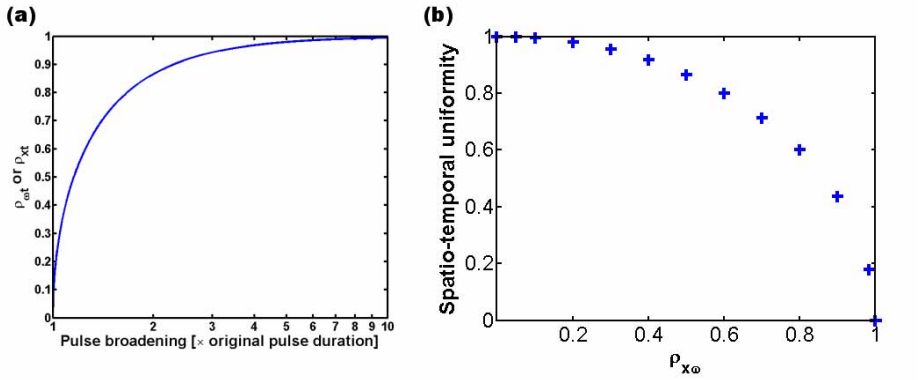

Fig. 4. (a) Normalized temporal chirp parameter $\rho_{\omega t}$ as a function of pulse broadening. Because pulse-front tilt also results in pulse broadening, this curve can also represent ρ_{xt}, as well as $\rho_{x\omega}$ if pulse broadening is replaced by beam magnification along x. (b) Numerical simulations of the degree of spatio-temporal uniformity μ as a function of the spatial chirp parameter $\rho_{x\omega}$ in the case of a Gaussian beam.

Due to the analogy between spatial and temporal chirp, it seems logical to impose equivalent tolerances on $\rho_{\omega t}$ and $\rho_{x\omega}$. In practice, $|\rho| \leq 0.30$ or 0.40 seems a reasonable condition to aim for. These considerations are also valid for the parameters ρ_{xt}, $\rho_{k\omega}$ and ρ_{kt}, which can be used to measure pulse-front tilt, angular dispersion, and angular delay, respectively, as long as the intensity distributions $I(x,t)$, $I(k_x,\omega)$ and $I(k_x,t)$ are known:

#77118 - $15.00 USD Received 15 November 2006; revised 15 December 2006; accepted 18 December 2006

$$\rho_{xt} \equiv \frac{\iint dxdtI(x,t)xt}{\Delta x \Delta t} \text{ (pulse-front tilt)}$$
$$\rho_{k\omega} \equiv \frac{\iint dkd\omega I(k_x,\omega)k_x\omega}{\Delta k_x \Delta \omega} \text{ (angular dispersion)} \quad (12)$$
$$\rho_{kt} \equiv \frac{\iint dkdtI(k_x,t)k_x t}{\Delta k_x \Delta t} \text{ (angular delay)}$$

At least to some extent, all of these spatio-temporal distortions are present at the same time in real pulses. It is an experimental challenge to control all these distortions, especially considering the fact that they are often entangled. Pulse-front tilt, for example, can be caused by angular dispersion [19] or simultaneous spatial and temporal chirp [20]. In the latter scenario, it is possible to derive an exact expression for pulse-front tilt in the ideal case of Gaussian pulses and beams: $dt/dx = (d\tau/d\omega)\cdot(d\omega/dx)$. This formula can be expressed in terms of normalized ρ-parameters as well: $\rho_{xt} = \rho_{x\omega}\cdot\rho_{\omega t}$ (see Fig. 6 for an example). For more complex pulses however, closed-form expressions for relationships between spatio-temporal distortions become difficult to establish, and from a practical point of view it is preferable to aim at maintaining all the various ρ-parameters below a certain threshold (e.g., 0.30) that eventually depends on the overall spatio-temporal pulse quality that is sought.

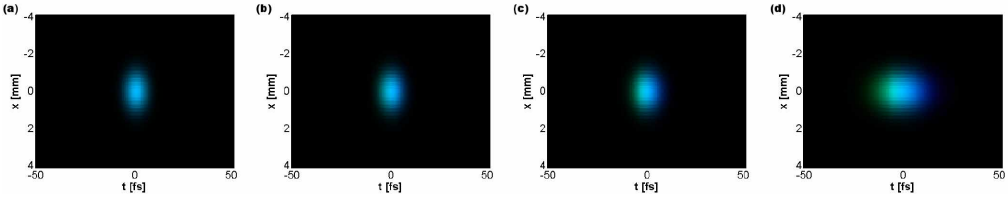

Fig. 5. Temporal profiles of an ultrashort pulse with increasing amounts of positive temporal chirp, and hence with increasing values of $\rho_{\omega t}$. The pulses have a central wavelength of 480 nm, and 35 nm of bandwidth. (a) $\rho_{\omega t} = 0.00$ (transform limit). (b) $\rho_{\omega t} = 0.30$ (5% broadening). (c) $\rho_{\omega t} = 0.60$ (25% broadening). (d) $\rho_{\omega t} = 0.90$ (130% broadening).

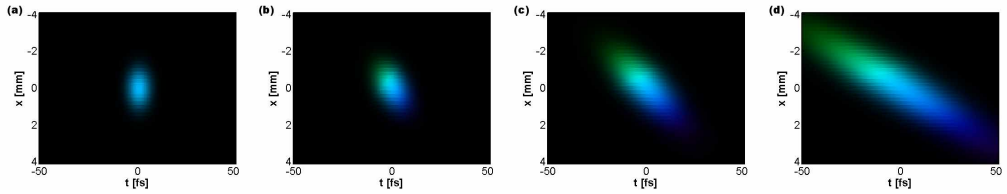

Fig. 6. Spatio-temporal profiles of an ultrashort pulse with increasing amounts of temporal and spatial chirp, and hence with increasing values of ρ_{xt}. The pulses have a central wavelength of 480 nm, and 35 nm of bandwidth. (a) $\rho_{xt} = 0.00$. (b) $\rho_{xt} = 0.30$. (c) $\rho_{xt} = 0.60$. (d) $\rho_{xt} = 0.80$.

Finally, we would like to point out that the ρ-parameters also seem to offer the possibility to describe spatio-temporal distortions beyond the first order, such as chromatic aberrations in lenses, or pulse-front curvature, by considering higher-order cross moments μ_{pq} of the relevant intensity distributions.

#77118 - $15.00 USD Received 15 November 2006; revised 15 December 2006; accepted 18 December 2006

6. Conclusions

We have presented an intuitive description of various spatio-temporal distortions in terms of a set of normalized correlation coefficients. Spatial chirp, pulse-front tilt, angular dispersion and angular delay, and also temporal chirp, can all be described to first order by dimensionless parameters that vary in the range [-1,1] and readily indicate the *severity* of these distortions. These parameters are especially sensitive to small amounts of distortion. We also presented a simple, practical apparatus allowing the real-time monitoring of the corresponding spatial-chirp parameters $\rho_{x\lambda}$ and $\rho_{y\lambda}$,. We believe that these parameters will help better understand spatio-temporal distortions and their consequences, and will be used as a benchmark enabling the comparison of the performance of ultrafast lasers.

Acknowledgments

This work was funded by an endowment provided by the Georgia Research Alliance.

#77118 - $15.00 USD Received 15 November 2006; revised 15 December 2006; accepted 18 December 2006